

# A potent sphingomyelinase inhibitor from *Cordyceps* mycelia contributes its cytoprotective effect against oxidative stress in macrophages<sup>S</sup>

Shwu-Huey Wang,<sup>\*,†</sup> Wen-Bin Yang,<sup>§</sup> Yin-Chen Liu,<sup>§</sup> Yi-Hua Chiu,<sup>†</sup> Chien-Tsu Chen,<sup>\*\*</sup> Pai-Feng Kao,<sup>††</sup> and Chun-Mao Lin<sup>1,\*\*,§§</sup>

Graduate Institute of Medical Sciences,<sup>\*</sup> Taipei Medical University, Taipei, Taiwan, Republic of China; Core Facility Center,<sup>†</sup> Office of Research and Development, Taipei Medical University, Taipei, Taiwan, Republic of China; Genomics Research Center,<sup>§</sup> Academia Sinica, Taipei, Taiwan, Republic of China; School of Medicine,<sup>\*\*</sup> Taipei Medical University, Taipei, Taiwan, Republic of China; Division of Cardiology,<sup>††</sup> Wan Fang Hospital, Taipei, Taiwan, Republic of China; and Orthopedics Research Center,<sup>§§</sup> Taipei Medical University Hospital, Taipei, Taiwan, Republic of China

**Abstract** A novel water-soluble polysaccharide fraction, CME-1, with a molecular mass of 27.6 kDa and containing mannose and galactose in a respective ratio of 4:6, was prepared from *Cordyceps sinensis* mycelia and identified by NMR and GC-MS. In the current study, we examined whether CME-1 has anti-inflammatory effects in RAW264.7 cells. The ability of CME-1 to inhibit H<sub>2</sub>O<sub>2</sub>-induced cell death in RAW264.7 cells was assessed by using an MTT assay and annexin V/propidium iodide double staining; we found that CME-1 protected cells against H<sub>2</sub>O<sub>2</sub>-induced injury. H<sub>2</sub>O<sub>2</sub>-induced intracellular oxidative stress and mitochondrial membrane depolarization were also diminished with CME-1 treatment. We evaluated the hydroxyl radical scavenging ability of CME-1 by using the DMPO-electron spin resonance technique, which indicated that CME-1 acts as an intracellular antioxidant in a concentration-dependent manner through a mechanism other than its scavenging activity. Activities of both neutral and acid sphingomyelinases (SMases) were assessed in vitro, and results showed that the CME-1 inhibited activities of both neutral and acid SMases in a concentration-dependent manner. CME-1 reduced H<sub>2</sub>O<sub>2</sub> treatment-elevated C16- and C18-ceramide levels measured by LC/MS/MS in RAW264.7 cells. **Results suggest that CME-1 protects RAW264.7 cells against oxidative stress through inhibition of SMase activity and reduction of C16- and C18-ceramide levels.**—Wang, S-H., W-B. Yang, Y-C. Liu, Y-H. Chiu, C-T. Chen, P-F. Kao, and C-M. Lin. **A potent sphingomyelinase inhibitor from *Cordyceps* mycelia contributes its cytoprotective effect against oxidative stress in macrophages.** *J. Lipid Res.* 2011. 52: 471–479.

**Supplementary key words** ceramide • *Cordyceps sinensis* mycelia • macrophage • polysaccharide • reactive oxygen species • sphingomyelin

This study was supported by grants from the National Science Council (NSC99-2313-M-038-001) and Taipei Medical University-Wan Fang Hospital (98TMU-WFH-03-2), Taiwan.

Manuscript received 5 September 2010 and in revised form 30 November 2010.

Published, JLR Papers in Press, January 7, 2011  
DOI 10.1194/jlr.M011015

*Cordyceps sinensis* (CS) has been commonly used recently to affect the nervous system, glucose metabolism, inflammatory conditions, cancer, kidney diseases, and respiratory, hepatic, and cardiovascular immunologic diseases (1). *Cordyceps* mycelia (CM) extract is a promising source of therapeutic medicines because it can be mass-produced and it has a chemical composition similar to that of the fruiting body of CS (2). The inhibitory effect that mycelial extract has on liposome oxidation was superior to that of the fruiting body; and levels of polyphenolics and bioactive components in the mycelial extract were also higher than those in the fruiting body (3). A number of bioactive constituents from *Cordyceps* species have been reported (4), including cordycepin, antibacterial and antitumor adenosine derivatives, sterols, polyphenolics, and polysaccharides. Polysaccharides isolated from *Cordyceps* species are major antioxidant phytochemicals and have been shown to have anti-inflammatory, antitumor, and immunomodulatory activities (5). Akaki et al. (6) reported the effects of polysaccharides from cultured mycelia on high tumor necrosis

Abbreviations: aSMase, acidic sphingomyelinase; CM, *Cordyceps* mycelia; CME-1, a polysaccharide from the water-soluble fraction of *Cordyceps sinensis* mycelia; CS, *Cordyceps sinensis*; DCFDA, 2,7-dichlorofluorescein diacetate; DMPO, 5-dimethyl-1-pyrroline-*N*-oxide; DOSY NMR, diffusion ordered spectroscopy NMR; ESR, electron spin resonance; FACS, fluorescence-activated cell sorting; GW4869, *N,N*-Bis[4-(4,5-dihydro-1H-imidazol-2-yl)phenyl]-3,3'-*p*-phenylene-bis-acrylamide dihydrochloride; HPAEC-PAD, high-performance anion-exchange chromatography with pulsed amperometric detection; HPLC, high-performance liquid chromatography; JC-1, 5,5',6,6'-tetrachloro-1,1',3,3'-tetraethylbenzimidazolyl carbocyanine iodide; MTT, 3-(4,5-dimethylthiazol-2-yl)-2,5-diphenyl tetrazolium bromide; nSMase, neutral SMase; PI, propidium iodide; ROS, reactive oxygen species; SM, sphingomyelin; TNF- $\alpha$ , tumor necrosis factor- $\alpha$ ; XO, xanthine oxidase.

<sup>1</sup>To whom correspondence should be addressed.

e-mail: cmlin@tmu.edu.tw

<sup>S</sup>The online version of this article (available at <http://www.jlr.org>) contains supplementary data in the form of five figures.

factor- $\alpha$  (TNF- $\alpha$ )-producing activities in RAW264.7 cells. However, it was stated that it is necessary to elucidate the chemically uncharacterized polysaccharide extracts and determine their pharmacological mechanisms (5).

Oxidative stress is implicated in a great variety of physiological and pathological processes (7). The toxicity ascribed to superoxide radicals is believed to be caused by superoxide's direct interaction with biological targets. A wide range of toxic oxidative reactions are initiated by reactive oxygen species (ROS) (8) and released by phagocytic cells, which are involved in phagocytosis. Excessive and persistent formation of ROS by inflammatory cells is thought to be a key factor in genotoxic effects. Administration of antioxidants can produce potential benefits by attenuating injury caused by oxidative stress, and attempts have been made to screen for natural antioxidant agents.

Sphingomyelinase (SMase) is expressed by almost all cell types and is localized in phagosomes, endosomes, lysosomes, and plasma membranes (9). Elevated intracellular ceramide production is induced predominantly by the elevated hydrolytic activity of SMases. Ceramide is an intracellular lipid mediator that responds to stress and various stimuli and is involved in various signaling pathways associated with cell cycle regulation, differentiation, senescence, and apoptosis (10, 11). Many reports have indicated that signal transduction through sphingomyelin (SM) and ceramide strongly affects the immune response, either directly through cell signaling events or indirectly through cytokines produced by other cells as the result of signaling through the SM pathway (12). Sphingolipid signal transduction pathways also play important roles in regulating atherosclerosis pathogenesis through modulating the fate of macrophages (13). The inflammatory oxidant, H<sub>2</sub>O<sub>2</sub>, induces rapid elevation of ceramide from the hydrolysis of SM in plasma membranes, which contributes to apoptosis induction in epithelial cells (14). Herein, in addition to describing our study of the structure of CME-1, a water-soluble polysaccharide extract from CM, we further demonstrate that the action of CME-1 is capable of interfering with SMases, and we outline the potential implications for medicinal chemistry.

## MATERIALS AND METHODS

### Materials

Cultured CM was purchased from GeneFerm Biotechnology (Tainan, Taiwan). Hydrogen peroxide (H<sub>2</sub>O<sub>2</sub>); 3-(4,5-dimethylthiazol-2-yl)-2,5-diphenyl tetrazolium bromide (MTT); 2,7-dichlorofluorescein diacetate (DCFDA); and 5-dimethyl-1-pyrroline-N-oxide (DMPO) were purchased from Sigma Chemical (St. Louis, MO). All solvents used in this study were from Merck (Darmstadt, Germany). Dulbecco's modified Eagle's medium (DMEM), penicillin, and streptomycin were obtained from Gibco BRL (Grand Island, NY). Antibodies for Western blot analysis were from Cell Signaling Technology (Danvers, MA). An annexin V-FITC apoptosis detection kit and a kit for flow cytometry detection of mitochondrial membrane potential were purchased from Becton Dickinson (Biosciences, San Diego, CA). An SMase assay kit was purchased from Invitrogen (Carlsbad, CA).

### Preparation of polysaccharides from *Cordyceps* mycelia

Cultured CM was extracted from dried powder (200 g) by using double-distilled H<sub>2</sub>O (200 ml) three times for 3 h at room temperature (25°C). Extracts were combined and concentrated to give 65 g (33%) of crude residue (water-soluble fraction of *Cordyceps sinensis* mycelia [CME]). Two grams of CME were fractionated by gel filtration column chromatography (Sephacryl G-15 column; 2.5 × 45 cm) with the double-distilled H<sub>2</sub>O eluent, which yielded the polysaccharide CME-1 (12%). The CME-1 fraction was collected using the phenol-sulfuric acid method, and the absorption was read at 490 nm (15). For the polysaccharide composition analysis, fractions were hydrolyzed in 4 M trifluoroacetic acid at 112°C for 8 h, and the hydrolysate was measured with high-performance anion-exchange chromatography with pulsed amperometric detection (HPAEC-PAD), using an ICS-3000 ion chromatography system (Dionex, Sunnyvale, CA). The hydrolysate was eluted with a mixture of water and 200 mM NaOH in a volume ratio of 92:8, through a CarboPac PA-10 column (2 × 250 mm; Sunnyvale, CA). Molecular masses of the fractions were predicted using a diffusion ordered spectroscopy (DOSY) experiment (AV600 NMR spectrometer; Bruker, Rheinstetten, Germany) (16). The chemical structure of CME-1 was determined according to a previous report (17) and by using a GC-MS profile.

### Cell culture

The mouse monocyte-macrophage cell line, RAW 264.7, was cultured in DMEM supplemented with 10% FBS, 100 U/ml penicillin, and 100 mg/ml streptomycin. Conditions were maintained in a humidified incubator (95% air with 5% CO<sub>2</sub>) at 37°C.

### Cell viability assay

An MTT assay was performed to test cytotoxicity and cell viability, as described previously (18), based on the conversion of yellow tetrazolium salt to purple formazan product. Cells (1 × 10<sup>5</sup> cells/ml) were grown on a 96-well plate, supplemented with culture medium. Cells were treated with CME-1 (0–150 µg/ml) or with CME-1 combined with 200 µM H<sub>2</sub>O<sub>2</sub> for 24 h, after which an MTT solution (1 mg/ml in PBS) was added, and cells were incubated for 2 h. After the supernatant was eliminated and DMSO was added to the well, the absorbance at 570 nm was measured with a spectrophotometer (Thermo Varioskan Flash, Vantaa, Finland).

### Detection of cell death

Cells undergoing death were measured by an annexin V-FITC and propidium iodide (PI)-dual staining kit. Briefly, 2 × 10<sup>5</sup> cells were treated with 200 µM H<sub>2</sub>O<sub>2</sub> in the presence or absence of CME-1 for 24 h; cells were then detached, pelleted, washed in PBS, and resuspended in binding buffer containing the conjugated annexin V (annexin V-FITC) and PI for 15 min according to the manufacturer's protocol. These cell samples were analyzed using a fluorescence-activated cell sorting (FACS)Canto-II flow cytometer (BD Biosciences, San Jose, CA). The Q1, Q2, and Q4 regions that were positive for either annexin V or PI corresponded to cell death (19). Annexin V- and PI-negative cell populations that appeared in the Q3 region were normal cells.

### Measurement of intracellular ROS generation

Levels of cellular oxidative stress were measured using the fluorescent probe, DCFDA, as described previously (20). After being treated with 200 µM H<sub>2</sub>O<sub>2</sub> in the absence or presence of CME-1 (100 µg/ml), RAW264.7 cells were treated with 20 µM DCFDA for 10 min and then washed in PBS. DCFDA is trapped mainly in the cytoplasm and is oxidized to the highly fluorescent dichlorofluorescein (DCF) by intracellular ROS. The DCF fluorescence

intensity of cells was measured with a fluorescence spectrometer (Thermo Varioskan Flash) and imaged using fluorescence microscopy (Olympus IX71, Tokyo, Japan).

### Measurement of the mitochondrial membrane potential

The loss of mitochondrial membrane potential ( $\Delta\psi_m$ ) is a hallmark of cell death. RAW264.7 cells ( $1.0 \times 10^5$  cells/ml) were grown until the desired confluence level was reached and treated with 200  $\mu\text{M}$   $\text{H}_2\text{O}_2$  and CME-1 for 24 h. Cells were then exposed to 5  $\mu\text{g}/\text{ml}$  JC-1 (5,5',6,6'-tetrachloro-1,1',3,3'-tetraethylbenzimidazolylcarbocyanine iodide) dye solution (mitochondrial membrane potential detection kit) for 15 min at 37°C, and cells showing JC-1 fluorescence were analyzed with a FACSCantoII flow cytometer (BD Biosciences, San Jose, CA). The JC-1 dye undergoes a reversible change in fluorescence emission from green to red as the  $\Delta\psi_m$  increases. Normal cells with a high  $\Delta\psi_m$  value promote aggregation of the JC-1 dye in mitochondria, which shifts the emission of the dye to the red spectral region (FITC-A, P1). However, cells with low  $\Delta\psi_m$  value do not induce JC-1 to aggregate; thus, the emission of the dye remains in the green spectral region (PE-A, P2). The ratio of the red/green fluorescence intensities (P1:P2) reflects changes in the  $\Delta\psi_m$  (21).

### Electron spin resonance trapping assay

Inhibition of iron-induced hydroxyl radical formation was determined using the electron spin resonance (ESR) trapping technique in combination with DMPO. The DMPO-OH adduct was obtained from the Fenton reaction system containing 100 mM DMPO, 10  $\mu\text{M}$   $\text{H}_2\text{O}_2$ , and 50  $\mu\text{M}$  ferrous ammonium sulfate with or without CME-1. The mixture was transferred to a flat quartz cell, and the ESR spectrum was measured 30 s after the addition of ferrous ammonium sulfate. The spin adducts generated in the reaction system were detected using an EMX-6/1 ESR spectrometer (Bruker, Karlsruhe, Germany) (18). Instrument conditions were as follows: a central magnetic field of 3,482 gauss (G); an X-band modulation frequency of 100 kHz; a power of 10.08 mW; a modulation amplitude of 2 G; a time constant of 2.56 ms; and a sweep time of 10.49 s. ESR spectra were measured at room temperature. The intensities of the DMPO-OH spin adduct were evaluated by comparing the peak intensities.

### Inhibition of neutral and acidic SMase activities by CME-1

Neutral SMase (nSMase) activity was measured using an Amplex Red SMase assay kit (Invitrogen) according to procedures described by the manufacturer. Briefly, the assay mixture contained the following components in a total volume of 200  $\mu\text{l}$ : 100  $\mu\text{l}$  of the enzyme source (0.04 units/ml SMase, 1 unit/ml HRP, 0.2 units/ml choline oxidase, 8 units/ml alkaline phosphatase, and 500  $\mu\text{M}$  SM at pH 7.4) in the absence or presence of CME-1 (0–200  $\mu\text{g}/\text{ml}$ ). Assay mixtures were incubated at 37°C for 30 min for the nSMase assay. The assay of acidic SMase (aSMase) activity was performed at pH 5.0. The reaction mixture contained 0.4 units/ml SMase, CME-1 (0–200  $\mu\text{g}/\text{ml}$ ), and 500  $\mu\text{M}$  SM in 100  $\mu\text{l}$  of 50 mM sodium acetate, pH 5.0, and cell samples were incubated at 37°C for 30 min. A 100- $\mu\text{l}$  working solution (consisting of 100  $\mu\text{M}$  Amplex Red, 1 unit/ml HRP, 0.2 units/ml choline oxidase, and 8 units/ml alkaline phosphatase in 100 mM Tris-HCl [pH 8.0]) was added, and cells were incubated at 37°C for 30 min. Fluorescence was measured with a microplate reader (Thermo Varioskan Flash) with excitation at 545 nm and emission at 585 nm.

### Cytoprotective effect of SMase inhibitors in $\text{H}_2\text{O}_2$ -treated cells

Cells ( $1 \times 10^5$  cells/ml) were grown on a 96-well plate, supplemented with culture medium. Cells were pretreated with GW4869

(0–3  $\mu\text{M}$ ) or imipramide (0–10  $\mu\text{M}$ ) for 5 min at room temperature.  $\text{H}_2\text{O}_2$  (200  $\mu\text{M}$ ) was added to the cell solution, and the culture was incubated for a further 24 h. Cell viability was estimated by using an MTT assay as described above.

### Quantification of ceramide

Ceramide levels of RAW264.7 cells were measured as described previously (22). Cells were treated with  $\text{H}_2\text{O}_2$  (200  $\mu\text{M}$ ) in the presence or absence of CME-1 (100  $\mu\text{g}/\text{ml}$ ) for 0.5–6 h. Cells were counted in a Neubauer counting chamber and harvested by centrifugation at 745  $g$  at 4°C for 5 min. The lipid fractions were extracted with 200- $\mu\text{l}$  solution of methanol to which internal standards (C17:0-ceramide) had been added. After vigorous agitation, the solution was centrifuged at 25,000 rpm for 10 min at 4°C, and the supernatants were collected.

The organic phases were assayed to quantify the amounts of C16:0-, C18:0-, C24:0-, and C24:1-ceramide, using liquid chromatography coupled with tandem mass spectrometry (LC/MS/MS). Chromatographic separation was achieved under gradient conditions using a Luna C18 column (150- $\times$  2-mm inner diameter; 5- $\mu\text{m}$  particle size; 10-nm pore size). High-performance liquid chromatographic (HPLC) mobile phases consisted of water-formic acid (100:0.1, v/v) and acetonitrile-tetrahydrofuran-formic acid (50:50:0.1, v/v/v). A gradient program was used for HPLC separation at a flow rate of 0.3 ml/min. Tandem MS analyses were performed with an API 4000 triple quadrupole MS unit with a Turbo V source (Applied BioSystems, MDS Sciex, Toronto, Canada). Precursor-to-product ion transitions of  $m/z$  536.8  $\rightarrow$  280.5 for C16:0-ceramide;  $m/z$  564.9  $\rightarrow$  308.5 for C18:0-ceramide;  $m/z$  646.9  $\rightarrow$  390.8 for C24:1-ceramide;  $m/z$  648.9  $\rightarrow$  392.8 for C24:0-ceramide; and  $m/z$  550.9  $\rightarrow$  294.5 for C17:0-ceramide were used to monitor multiple reactions with a dwell time of 15 ms. Concentrations of the calibration standards, quality controls, and unknowns were evaluated with Analyst version 1.4.2 software (Applied BioSystems). Total ceramide was calculated from the sum of the C16:0-, C18:0-, C24:0-, and C24:1-ceramide subspecies.

### Statistical analysis

Data are represented as means  $\pm$  SD of three replicates, and at least three separate experiments were performed. Treatments and controls were compared with Student's *t*-test. A *P* value of  $<0.05$  was accepted as statistically significant.

## RESULTS

### CME-1, a novel polysaccharide, purified from cultured *Cordyceps mycelia*

The novel polysaccharide, CME-1, obtained from cultured *Cordyceps mycelia* was fractionated by gel filtration after water extraction. The properties of CME-1 were established. The molecular mass was determined by DOSY NMR (see supplementary Fig. 1), and the monosaccharide components were determined by HPAEC-PAD. **Table 1** shows that CME-1, with a molecular mass of 27.6 kDa, contained 95% carbohydrates and had a mannose/galactose/glucose composition ratio of 39.1:59.2:1.7. The structure was suggested to consist of a backbone possessing (1 $\rightarrow$ 4)-linked mannose with galactose branches attached to the O-6 of mannose (**Fig. 1**). Branches mainly linking (1 $\rightarrow$ 4)-galactose were deduced according to the molar ratios and GC-MS profile (see supplementary Fig. II).



TABLE 1. Molecular mass, components of monosaccharide, and properties of CME-1

Component	CME-1
$[\alpha]_D^{20}$	$-20.6^\circ$
Molecular mass	27.6 kDa
Monosaccharide component ratio <sup>a</sup>	
Mannose	39.1 mol
Galactose	59.2 mol
Glucose	1.7 mol

<sup>a</sup>Analyzed by HPAEC-PAD.

### Protective effects of CME-1 against H<sub>2</sub>O<sub>2</sub>-induced RAW264.7 cell death

The extent of the cytotoxicity of CME-1 to RAW264.7 cells was measured using an MTT assay (Fig. 2A). CME-1 did not show significant cytotoxicity toward RAW264.7 macrophages treated at 0–150  $\mu\text{g/ml}$  for 24 h. We utilized CME-1 to study its protective effect against H<sub>2</sub>O<sub>2</sub> injury. After cells were treated with H<sub>2</sub>O<sub>2</sub> (200  $\mu\text{M}$ ) for 24 h, cell viability was approximately 50%, according to an MTT assay, which was reversed to 100% when cells were cotreated with CME-1 (100  $\mu\text{g/ml}$ ) (Fig. 2B). CME-1 displayed a concentration-dependent protective effect against H<sub>2</sub>O<sub>2</sub> injury of RAW264.7 cells. The ability of CME-1 to inhibit H<sub>2</sub>O<sub>2</sub>-induced cell death of RAW264.7 cells was assessed using double staining with annexin V-FITC and PI. Annexin V and PI fluorescence intensities in untreated control cells were retained mostly in the Q3 region (which indicates normal cells) (Fig. 2C, left panel), whereas the proportion of cells increased in the Q2 region with H<sub>2</sub>O<sub>2</sub> treatment (200  $\mu\text{M}$ ) for 24 h (Fig. 2C, middle panel). The combination treatment with CME-1 obviously reduced the percentage in the Q2 region compared with that of H<sub>2</sub>O<sub>2</sub> treatment only (Fig. 2C, right panel). A statistical analysis of the cell population percentage in the Q1 plus Q2 plus Q4 regions (cell death region) in Fig. 2C is shown in Fig. 2D. H<sub>2</sub>O<sub>2</sub> induced an increase in annexin V/PI-positive cells from 10% in control cells to 100%, and cotreatment with CME-1 decreased the percentage from 100% with H<sub>2</sub>O<sub>2</sub> treatment to 60%. These data suggest that CME-1 possesses the ability to protect cells against H<sub>2</sub>O<sub>2</sub>-induced cell death in a concentration-dependent manner.

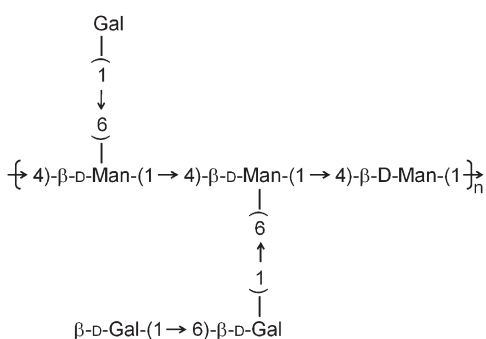


Fig. 1. The structure of CME-1 is shown, with a backbone possessing (1→4)-linked mannose and galactose branches attached to the O-6 of mannose.

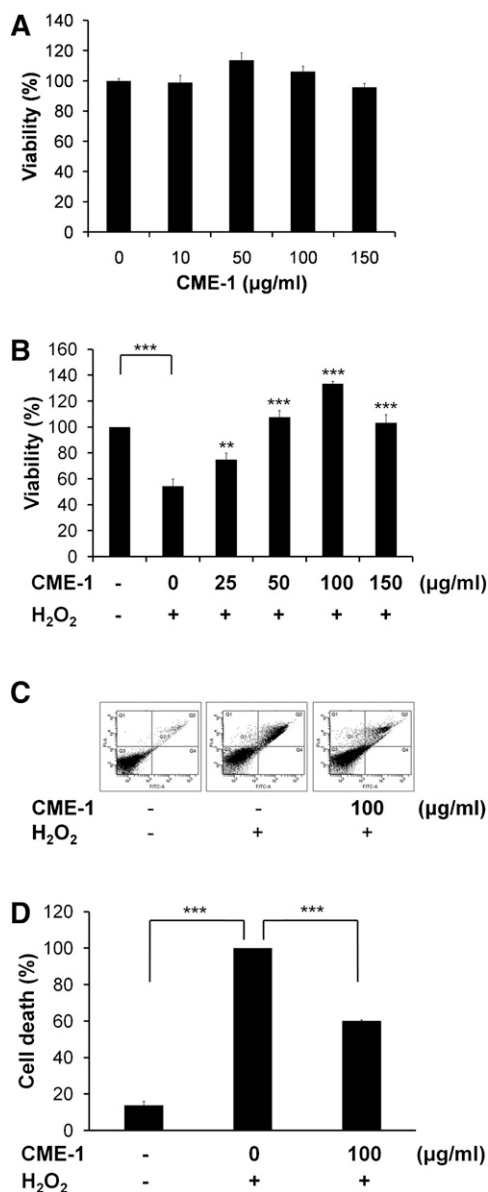


Fig. 2. Protective effects of CME-1 against H<sub>2</sub>O<sub>2</sub>-induced cytotoxicity in RAW264.7 cells. A: The cytotoxicity of CME-1 to RAW264.7 cells was measured using an MTT assay. Cells were treated with CME-1 (at 0, 10, 50, 100, and 150  $\mu\text{g/ml}$ ) for 24 h. Results are presented as means  $\pm$  SD for  $n = 3$  replicates. B: The protective effect of CME-1 on H<sub>2</sub>O<sub>2</sub>-induced cytotoxicity in RAW264.7 cells is shown. Cells were cotreated with H<sub>2</sub>O<sub>2</sub> (200  $\mu\text{M}$ ) and CME-1 (0, 25, 50, 100, and 150  $\mu\text{g/ml}$ ) for 24 h. Results are presented as the means  $\pm$  SD for  $n = 3$  replicates; \*\*,  $P < 0.01$ ; \*\*\*,  $P < 0.001$ , compared with H<sub>2</sub>O<sub>2</sub> treatment alone. C: Cell death was detected by flow cytometry with annexin V/PI-double staining upon cell treatment for 24 h. Fractions of the annexin V- and PI-positive populations are indicated. D: Statistical analysis of the cell populations is shown. The percentage of dead cells (Q1 + Q2 + Q4) is presented, and data are presented as means  $\pm$  SD for  $n = 3$  replicates; \*\*\*,  $P < 0.001$ , compared with the group treated with only H<sub>2</sub>O<sub>2</sub>.

### CME-1 prevents H<sub>2</sub>O<sub>2</sub>-induced intracellular oxidative stress and mitochondrial membrane depolarization

H<sub>2</sub>O<sub>2</sub> treatment is known to induce intracellular oxidative stress by upregulating ROS production and mitochondrial membrane aberrations. We measured intracellular

ROS in RAW264.7 cells that had been exogenously challenged with H<sub>2</sub>O<sub>2</sub> (200 μM) for 30 min with and without co-incubation with CME-1. ROS formation was visualized by fluorescence microscopy with the redox-sensitive fluorescent dye DCFDA. Oxidized DCF fluorescence was significantly more intense in RAW264.7 cells treated with H<sub>2</sub>O<sub>2</sub> alone (Fig. 3A-b) than in untreated control cells (Fig. 3A-a). With CME-1 cotreatment, DCF fluorescence was remarkably decreased compared with that of H<sub>2</sub>O<sub>2</sub>-only treatment (Fig. 3A-c). We further quantified the amount of ROS generated by H<sub>2</sub>O<sub>2</sub> treatment for 24 h by DCF fluorescence, using a fluorescence spectrometer. The DCF fluorescence intensity of H<sub>2</sub>O<sub>2</sub>-treated cells was 1.45-fold increased compared with that of untreated control cells. In comparison, cells co-incubated with CME-1 (0–100 μg/ml) exhibited much lower levels of ROS (Fig. 3B). The increment of CME-1 reduced the amount of ROS in H<sub>2</sub>O<sub>2</sub>-treated RAW264.7 cells.

Oxidative stress is known to decrease the  $\Delta\Psi_m$  value, and a rise in the potential has significant effects on cell viability. We utilized JC-1 dye to track changes of  $\Delta\Psi_m$  value in H<sub>2</sub>O<sub>2</sub>-treated RAW264.7 cells in the presence and absence of CME-1. The P1 population, according to JC-1 accumulation in mitochondria, increased with CME-1 treatments by 50 and 100 μg/ml compared with that in cells treated with H<sub>2</sub>O<sub>2</sub> alone, respectively. (Fig. 3C). The P1/P2 ratio, reflecting the protective effect of membrane integrity, was 1.6 for H<sub>2</sub>O<sub>2</sub>-treated cells (Fig. 3C, left panel), which increased to 6.1 and 6.7 in the presence of 50 and 100 μg/ml CME-1, respectively. These data indicate that CME-1 protected cells against H<sub>2</sub>O<sub>2</sub>-induced mitochondrial depolar-

ization. The results are fully consistent with the results shown in Fig. 2, in which CME-1 prevented RAW264.7 cells from undergoing H<sub>2</sub>O<sub>2</sub>-induced cell death.

### CME-1 does not scavenge hydroxyl radicals

ESR technique was used to further verify that the CME-1 examined herein possessed the ability to scavenge hydroxyl radicals, and the results are shown in Fig. 4. DMPO is a spin trapping reagent that reacts with hydroxyl radicals to generate a DMPO-OH signal, and the spin resonance signal was quantified by ESR analysis. It was unclear whether the hydroxyl radical scavenging ability of CME-1 competed with DMPO for hydroxyl radicals, thus causing a diminution of the DMPO-OH signal. In the absence of CME-1, the Fenton reaction generated an ESR signal with a peak intensity of 805; under the same conditions, the peak intensity of the ESR signal was reduced to 417 in the presence of 400 μM caffeic acid (which was used as a positive control). CME-1 (at 100, 200, 500, and 1,000 μg/ml) did not markedly reduce the DMPO-OH signal intensity (Fig. 4), suggesting that CME-1 does not scavenge hydroxyl radicals at a high concentration, 1,000 μg/ml, under in vitro conditions. Equal amounts (1,000 μg/ml) of monomeric galactose and mannose in a ratio of 6:4 also did not show scavenging ability under the same conditions (see supplementary Fig. III). CME-1 expressed hydroxyl radical scavenging activity only at a very high concentration (30% inhibition at 7,000 μg/ml). This implies that CME-1 acts as an intracellular antioxidant in a concentration-dependent manner through a mechanism other than its hydroxyl radical scavenging activity.

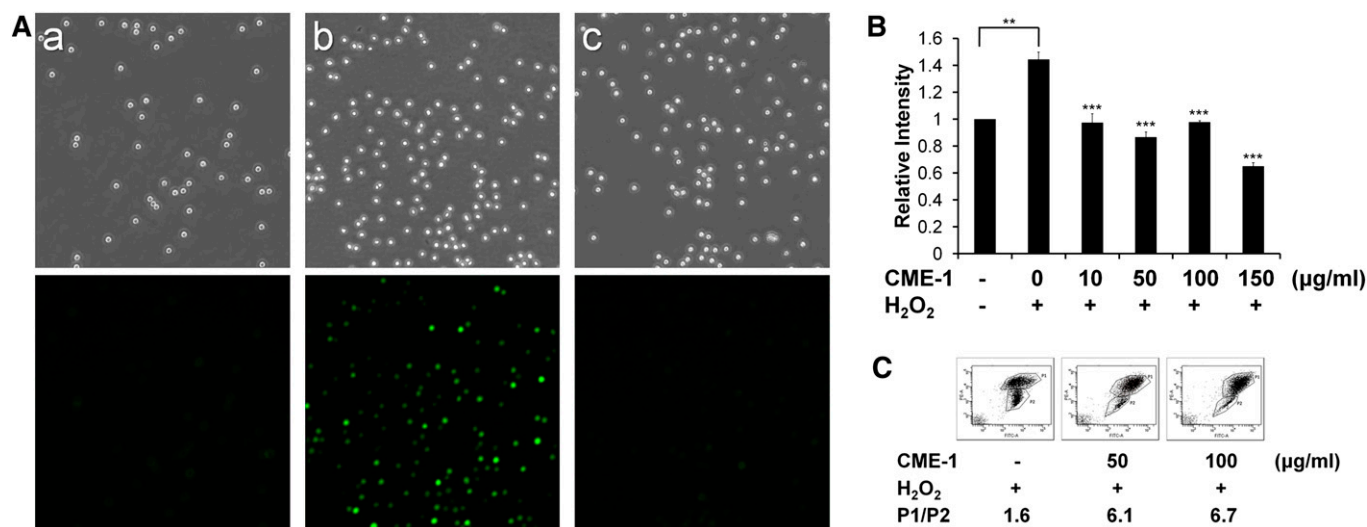


**Fig. 3.** CME-1 reduced H<sub>2</sub>O<sub>2</sub>-induced intracellular ROS levels and mitochondrial membrane depolarization. A: RAW264.7 cells were treated with H<sub>2</sub>O<sub>2</sub> (200 μM) and CME-1 (100 μg/ml) for 30 min, and intracellular ROS were measured using DCFDA fluorescence staining with fluorescence microscopy. (a) Untreated control, (b) H<sub>2</sub>O<sub>2</sub> treatment alone, and (c) cotreatment with H<sub>2</sub>O<sub>2</sub> and CME-1. Upper panels are images made with bright-field microscopy (original magnification 100×), and lower panels are images made with fluorescence microscopy. B: Cells were treated with H<sub>2</sub>O<sub>2</sub> with or without CME-1 (at 0, 10, 50, 100, and 150 μg/ml) for 24 h. After DCFDA staining, levels of intracellular ROS were quantified by a fluorometer, with excitation at 490 nm and emission at 530 nm. Relative intensities are presented as means ± SD for n = 3 replicates; \*\*, P < 0.01; \*\*\*, P < 0.001, compared with the group treated with only H<sub>2</sub>O<sub>2</sub>. C: Effects of CME-1 on changes in the mitochondrial membrane potential ( $\Delta\Psi_m$ ) were measured by JC-1 staining. Cell populations are presented using a dot plot with higher and lower JC-1-aggregated staining and gating, indicated as P1 and P2, respectively, and the P1/P2 ratio was calculated. Data shown are representatives of three independent experiments.

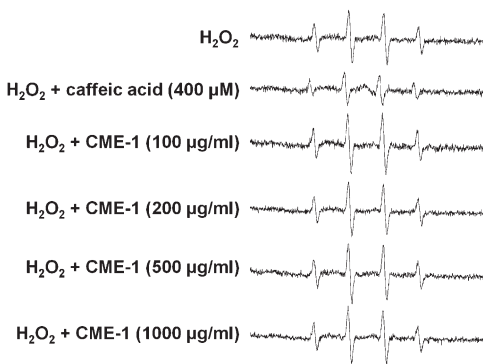


**Fig. 4.** Hydroxyl radical-scavenging activity of CME-1 measured by using DMPO-ESR. Hydroxyl radicals produced by the Fenton reaction were incubated with caffeic acid (400  $\mu\text{M}$ ) or CME-1 (at 0, 100, 200, 500, and 1,000  $\mu\text{g}/\text{ml}$ ) in the presence of DMPO (100 mM) and then detected with an ESR spectrometer. Data are representatives from three independent experiments.

### SMase activity inhibition by CME-1

Oxidative stress induces SMase activation, which is followed by promotion of ceramide production that induces cell death through ROS generation. To explore the effects of CME-1 against  $\text{H}_2\text{O}_2$  injury, we also examined a bacterial SMase activity assay *in vitro*. The activity of nSMase decreased along with an increase in CME-1 (0–200  $\mu\text{g}/\text{ml}$ ), with an  $\text{IC}_{50}$  value of approximately 50  $\mu\text{g}/\text{ml}$  (Fig. 5A). The kinetic assays showed a noncompetitive type of inhibition (data not shown). CME-1 also displayed an inhibitory effect on aSMase activity (Fig. 5B). These data suggested that CME-1 inhibited ROS production resulting from  $\text{H}_2\text{O}_2$  treatment, possibly through a decrease in SMase activity in cells. The amounts of cell protection against  $\text{H}_2\text{O}_2$ -induced damage afforded by the nSMase inhibitor GW4869 and the aSMase inhibitor imipramine were examined. As shown in Fig. 5C, after cells underwent  $\text{H}_2\text{O}_2$  treatment (200  $\mu\text{M}$ ) for 24 h, an MTT assay showed cell viability was about 50%, which was reversed in a statistically significant manner when RAW264.7 macrophage cells were pretreated with GW4869 (1–3  $\mu\text{M}$ ). Similar results were obtained with imipramine pretreatment (1–10  $\mu\text{M}$ ) (Fig. 5D). These results revealed that SMase inhibitors are able to protect cells against  $\text{H}_2\text{O}_2$ -induced damage and that CME-1 played a comparable role in SMase inhibition.

### CME-1 reduced ceramide levels elevated by $\text{H}_2\text{O}_2$ treatment

Ceramide is generated from hydrolysis of SM through the action of either aSMase or nSMase. For this reason, we tracked ceramide levels in cells after  $\text{H}_2\text{O}_2$  treatment with or without CME-1. Intracellular C16-, C18-, C24-, and C24:1-ceramides were quantified in RAW264.7 cells treated with  $\text{H}_2\text{O}_2$  for 0.5, 3, and 6 h, with or without CME-1, by using LC/MS/MS (see supplementary Fig. IV). C16- and C18-ceramides were significantly increased, 12- and 7-fold, respectively, after 6 h of  $\text{H}_2\text{O}_2$  treatment (Fig. 6), while C24- and C24:1-ceramide levels remained constant in response to  $\text{H}_2\text{O}_2$  treatment. Amounts of both C16- and C18-ceramides were approximately 2-fold decreased at 6 h after combined treatment with CME-1 (100  $\mu\text{g}/\text{ml}$ ). These

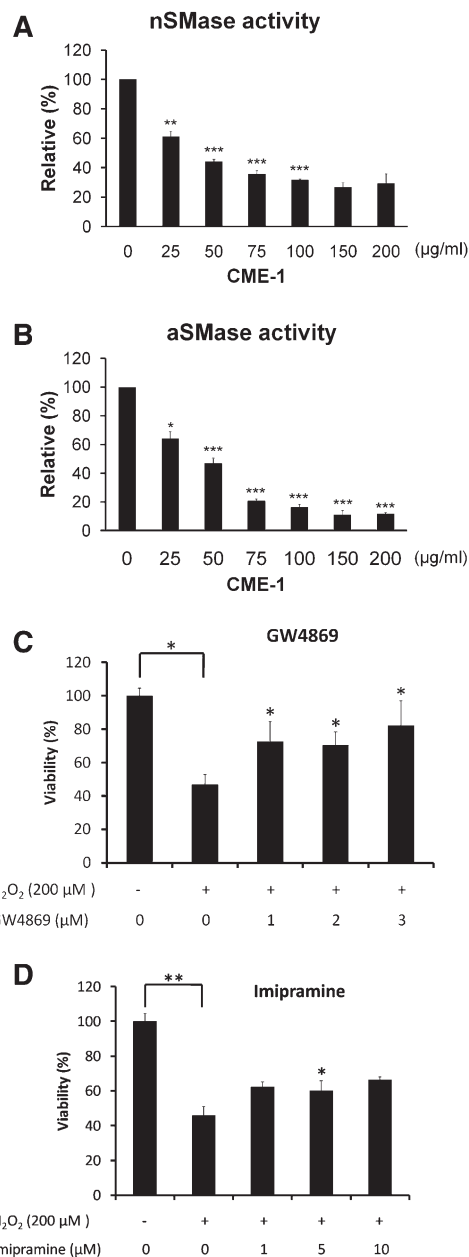


**Fig. 5.** Inhibition of SMase activity by CME-1 was determined with an Amplex red assay, as described in Materials and Methods. The relative activities of nSMase (A) and aSMase (B) of bacteria *in vitro* were measured after CME-1 treatment (at 0, 25, 50, 75, 100, 150, and 200  $\mu\text{g}/\text{ml}$ ) for 30 min. The relative activity is presented as the means  $\pm$  SD for  $n = 5$  replicates; \*,  $P < 0.05$ ; \*\*,  $P < 0.01$ ; \*\*\*,  $P < 0.001$ , compared with the untreated group. C: RAW264.7 cells were pretreated with GW4869 (0–3  $\mu\text{M}$ ) and (D) imipramine (0–10  $\mu\text{M}$ ) for 5 min, and then  $\text{H}_2\text{O}_2$  (200  $\mu\text{M}$ ) was added and cells were incubated for 24 h. Cell viability was determined with an MTT assay. Relative viability is presented as means  $\pm$  SD for  $n = 3$  replicates; \*,  $P < 0.05$ ; \*\*,  $P < 0.01$ , compared with the group treated with only  $\text{H}_2\text{O}_2$ .

results imply that CME-1 reduced  $\text{H}_2\text{O}_2$  treatment-elevated C16- and C18-ceramide levels in RAW264.7 cells.

## DISCUSSION

*Cordyceps* is a popular fungus used for herbal medicines in Asia. Polysaccharides extracted from *Cordyceps* have

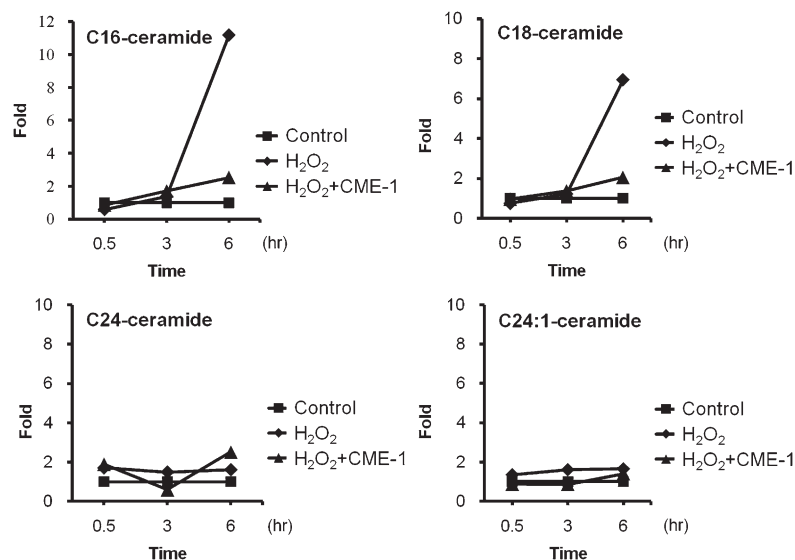


**Fig. 6.** CME-1 reduced H<sub>2</sub>O<sub>2</sub> treatment-elevated ceramide levels in RAW264.7 cells. Intracellular ceramide levels in RAW264.7 cells were detected in untreated (Control) cells, in cells with H<sub>2</sub>O<sub>2</sub> treatment (H<sub>2</sub>O<sub>2</sub>), and in cells cotreated with H<sub>2</sub>O<sub>2</sub> and CME-1 (H<sub>2</sub>O<sub>2</sub> + CME-1) for 0.5, 3, and 6 h. Various ceramide levels (C16-, C18-, C24:0-, and C24:1-ceramide) were measured by LC/MS/MS.

potency in improving apoptotic homeostasis and improving respiratory, renal, and cardiovascular functions (23). Polysaccharide extracts from *Cordyceps* might play important roles in modulating immune responses. Investigations of several innate immune receptors, including the macrophage mannose and galactose receptors, will be pursued in our future studies. Recently, hydrogen peroxide has increasingly been viewed as an important cellular paracrine that activates a variety of protein kinases and signaling pathways (24). Much oxidative stress can be overcome by cells' natural defenses; however, sustained stress can result in cell death. In our study, H<sub>2</sub>O<sub>2</sub>-induced cell death accompanied by mitochondrial depolarization was diminished by CME-1, while the proapoptotic protein Bax was downregulated with CME-1 treatment (data not shown). These results prompted us to investigate the immunomodulatory roles of CME-1 in H<sub>2</sub>O<sub>2</sub>-treated macrophage cells.

Polysaccharides from CM were found to have antioxidative, antiapoptotic (25), and anti-inflammatory activities (2). It has been reported that a polysaccharide extract from CS protected PC12 cells from H<sub>2</sub>O<sub>2</sub>-induced lipid peroxidation and cell death (25). The *in vitro* and intracellular radical scavenging ability was found to be associated with the biological effects. In our present investigation, CME-1 protected RAW264.7 cells against H<sub>2</sub>O<sub>2</sub>-induced cell death (Fig. 2B, C) and mitochondrial membrane aberrations (Fig. 3C). However, CME-1 did not show radical scavenging activity, according to the DMPO-ESR measurements (Fig. 4). CME-1 was estimated to scavenge H<sub>2</sub>O<sub>2</sub> at an optical density of 230 nm, and the result showed that CME-1 did not affect the absorption of H<sub>2</sub>O<sub>2</sub> at 230 nm within 5 min (data not shown). We suggest that the effects of CME-1 on H<sub>2</sub>O<sub>2</sub>-treated RAW264.7 cells are mediated through a mechanism other than scavenging activity.


Li et al. (26) extracted polysaccharides from cultured CM, using boiling water and ethanol. The first partially purified fraction of the water extract of cultured CM containing the largest amount of polysaccharides was analyzed for its anti-xanthine oxidase (XO) activity, which suggested that the activity was derived from *Cordyceps* polysaccharides. In

addition, these polysaccharides were found to have higher molecular masses (>200 kDa) and different sugar compositions than CME-1 (25). CME-1 in our study did not show distinct XO-inhibitory activity (see supplementary Fig. V), and it possessed a molecular mass of 27 kDa, which supports the probability that it had a composition distinct from that of the polysaccharide extracts described in the study by Li et al. (26).

Inflammatory factors, such as TNF- $\alpha$ , ROS, lipopolysaccharide (LPS) (27), amyloid- $\beta$  (28), interleukin-1 $\beta$  (IL-1 $\beta$ ) (29), and OX-low-density LDL (30), stimulated activation of SMase, which produced ceramide and formed a ceramide-rich platform from which to transmit death signaling. Sphingolipid-rich lipid rafts provide specialized lipid environments in which plasma membrane proteins regulate organization and functions, such as signaling cascades, protein and lipid sorting and trafficking, cell adhesion and migration, and immune responses (31). The lipid and protein compositions of lipid rafts have been reported to be associated with macrophage functions, such as polarized sorting of membrane proteins and signal transduction (32). Ceramide platforms are commonly formed in plasma membranes by the action of SMase upon hydrolysis of SM within lipid rafts. Elevated ceramide levels alter the membrane's physical properties and cause changes in fluidity, membrane composition, and surface pressure (33) that result in the transmission or amplification of transmembrane signals. SM, Toll-like receptor 4, and other members of the LPS receptor complex must be colocalized to the caveolar/lipid raft region for effective LPS signaling. Walton et al. (34) reported a pathway where LPS induction of IL-8 was inhibited by the activation of nSMase, which resulted in a change in the caveolin/lipid raft fraction. The formation of ceramide-enriched membrane domains makes important contributions to oxidative stress, which has major involvement in inflammation, immune responses, and phagocytosis of macrophages (35). In addition, ceramide induces activation of ROS-generating enzymes, including XO, NADPH oxidase, NO synthase, and the mitochondrial respiratory chain in a variety of



mammalian cells, including aortic smooth muscle cells, endothelial cells, and macrophages (36). Lipid raft disruption might be caused by SMase inhibitors, such as CME-1, that diminish the signaling transmitted from the ceramide platform. The reduced ceramide level might also attenuate activation of ROS-generating enzymes.

Mansat-de Mas et al. (37) demonstrated the involvement of the SM–ceramide cycle in anthracycline-induced apoptosis. ROS caused early ceramide generation through nSMase stimulation, and this was inhibited by antioxidants, which led to a decrease in ROS generation and apoptosis. This implies that a ceramide-mediated ROS production regulates H<sub>2</sub>O<sub>2</sub>-induced apoptosis by blocking the SM–ceramide signaling cascade in U937 cells (38). ROS play important roles in the SM–ceramide apoptotic pathway, which explains the novel mechanism of SMase inhibition against oxidative stress by CME-1. In our study, we found that CME-1 inhibited nSMase and aSMase activities in vitro (Fig. 5) and blocked C16- and C18-ceramide generation in RAW264.7 cells (Fig. 6). We suggest that protection of cells from H<sub>2</sub>O<sub>2</sub>-induced injury by CME-1 is mediated by decreased C16- and C18-ceramide levels resulting from SMase inhibition. In conclusion, we have demonstrated that the CM polysaccharide CME-1 protected RAW264.7 cells against H<sub>2</sub>O<sub>2</sub>-induced cell death. The effect was associated with SMase inhibitory activity through blockage of ceramide signaling, which suppressed intracellular ROS production and promoted normalization of the mitochondrial potential. 

Use of the API 4000 triple quadrupole mass spectrometer was supported by Yung Shin Pharmaceutical Co. (Taiwan).

## REFERENCES

- Zhu, J. S., G. M. Halpern, and K. Jones. 1998. The scientific rediscovery of an ancient Chinese herbal medicine: *Cordyceps sinensis*: part I. *J. Altern. Complement. Med.* **4**: 289–303.
- Yu, R., L. Song, Y. Zhao, W. Bin, L. Wang, H. Zhang, Y. Wu, W. Ye, and X. Yao. 2004. Isolation and biological properties of polysaccharide CPS-1 from cultured *Cordyceps militaris*. *Fitoterapia*. **75**: 465–472.
- Yu, H. M., B-S. Wang, S. C. Huang, and P-D. Duh. 2006. Comparison of protective effects between cultured *Cordyceps militaris* and natural *Cordyceps sinensis* against oxidative damage. *J. Agric. Food Chem.* **54**: 3132–3138.
- Wu, Y., H. Sun, F. Qin, Y. Pan, and C. Sun. 2006. Effect of various extracts and a polysaccharide from the edible mycelia of *Cordyceps sinensis* on cellular and humoral immune response against ovalbumin in mice. *Phytother. Res.* **20**: 646–652.
- Paterson, R. R. M. 2008. *Cordyceps*, a traditional Chinese medicine and another fungal therapeutic biofactory? *Phytochemistry*. **69**: 1469–1495.
- Akaki, J., Y. Matsui, H. Kojima, S. Nakajima, K. Kamei, and M. Tamesada. 2009. Structural analysis of monocyte activation constituents in cultured mycelia of *Cordyceps sinensis*. *Fitoterapia*. **80**: 182–187.
- Martindale, J. L., and N. J. Holbrook. 2002. Cellular response to oxidative stress: signaling for suicide and survival. *J. Cell. Physiol.* **192**: 1–15.
- Cuzzocrea, S., D. P. Riley, A. P. Caputi, and D. Salvemini. 2001. Antioxidant therapy: a new pharmacological approach in shock, inflammation, and ischemia/reperfusion injury. *Pharmacol. Rev.* **53**: 135–159.
- Utermöhlen, O., J. Herz, M. Schramm, and M. Krönke. 2008. Fusogenicity of membranes: the impact of acid sphingomyelinase on innate immune responses. *Immunobiology*. **213**: 307–314.
- Hannun, Y. A., and C. Luberto. 2000. Ceramide in the eukaryotic stress response. *Trends Cell Biol.* **10**: 73–80.
- Claus, R. A., M. J. Dorer, A. C. Bunck, and H. P. Deigner. 2009. Inhibition of sphingomyelin hydrolysis: targeting the lipid mediator ceramide as a key regulator of cellular fate. *Curr. Med. Chem.* **16**: 1978–2000.
- Melendez, A. J. 2008. Sphingosine kinase signalling in immune cells: potential as novel therapeutic targets. *Biochim. Biophys. Acta.* **1784**: 66–75.
- Steinbrecher, U. P., A. Gómez-Muñoz, and V. Duronio. 2004. Acid sphingomyelinase in macrophage apoptosis. *Curr. Opin. Lipidol.* **15**: 531–537.
- Goldkorn, T., N. Balaban, M. Shannon, V. Chea, K. Matsukuma, D. Gilchrist, H. Wang, and C. Chan. 1998. H<sub>2</sub>O<sub>2</sub> acts on cellular membranes to generate ceramide signaling and initiate apoptosis in tracheobronchial epithelial cells. *J. Cell Sci.* **111**: 3209–3220.
- Li, S. P., Z. R. Su, T. T. X. Dong, and K. W. K. Tsim. 2002. The fruiting body and its caterpillar host of *Cordyceps sinensis* show close resemblance in main constituents and anti-oxidation activity. *Phytomedicine*. **9**: 319–324.
- Viel, S., D. Capitani, L. Mannina, and A. Segre. 2003. Diffusion-ordered NMR spectroscopy: a versatile tool for the molecular weight determination of uncharged polysaccharides. *Biomacromolecules*. **4**: 1843–1847.
- Zhou, X., Z. Gong, Y. Su, J. Lin, and K. Tang. 2009. *Cordyceps* fungi: natural products, pharmacological functions and developmental products. *J. Pharm. Pharmacol.* **61**: 279–291.
- Lin, H-C., S-H. Tsai, C-S. Chen, Y-C. Chang, C-M. Lee, Z-Y. Lai, and C-M. Lin. 2008. Structure-activity relationship of coumarin derivatives on xanthine oxidase-inhibiting and free radical-scavenging activities. *Biochem. Pharmacol.* **75**: 1416–1425.
- Bergeron, M., J. K. A. Nicholson, S. Phaneuf, T. Ding, N. Soucy, A. D. Badley, N. C. Hawley Foss, and F. Mandy. 2002. Selection of lymphocyte gating protocol has an impact on the level of reliability of T-cell subsets in aging specimens. *Cytometry*. **50**: 53–61.
- Huang, S-H., C-M. Lin, and B-H. Chiang. 2008. Protective effects of *Angelica sinensis* extract on amyloid  $\beta$ -peptide-induced neurotoxicity. *Phytomedicine*. **15**: 710–721.
- Mantena, S. K., S. D. Sharma, and S. K. Katiyar. 2006. Berberine, a natural product, induces G1-phase cell cycle arrest and caspase-3-dependent apoptosis in human prostate carcinoma cells. *Mol. Cancer Ther.* **5**: 296–308.
- Chen, B-C., H-M. Chang, M-J. Hsu, C-M. Shih, Y-H. Chiu, W-T. Chiu, and C-H. Lin. 2009. Peptidoglycan induces cyclooxygenase-2 expression in macrophages by activating the neutral sphingomyelinase-ceramide pathway. *J. Biol. Chem.* **284**: 20562–20573.
- Hsu, T-L., S-C. Cheng, W-B. Yang, S-W. Chin, B-H. Chen, M-T. Huang, S-L. Hsieh, and C-H. Wong. 2009. Profiling carbohydrate-receptor interaction with recombinant innate immunity receptor-Fc fusion proteins. *J. Biol. Chem.* **284**: 34479–34489.
- Ardanaz, N., and P. J. Pagano. 2006. Hydrogen peroxide as a paracrine vascular mediator: regulation and signaling leading to dysfunction. *Exp. Biol. Med. (Maywood)*. **231**: 237–251.
- Li, S. P., K. J. Zhao, Z. N. Ji, Z. H. Song, T. T. Dong, C. K. Lo, J. K. Cheung, S. Q. Zhu, and K. W. Tsim. 2003. A polysaccharide isolated from *Cordyceps sinensis*, a traditional Chinese medicine, protects PC12 cells against hydrogen peroxide-induced injury. *Life Sci.* **73**: 2503–2513.
- Li, S. P., P. Li, T. T. Dong, and K. W. Tsim. 2001. Anti-oxidation activity of different types of natural *Cordyceps sinensis* and cultured *Cordyceps* mycelia. *Phytomedicine*. **8**: 207–212.
- Stancevic, B., and R. Kolesnick. 2010. Ceramide-rich platforms in transmembrane signaling. *FEBS Lett.* **584**: 1728–1740.
- Jana, A., and K. Pahan. 2010. Fibrillar amyloid- $\beta$ -activated human astroglia kill primary human neurons via neutral sphingomyelinase: implications for Alzheimer's disease. *J. Neurosci.* **30**: 12676–12689.
- Jenkins, R. W., D. Canals, J. Idkowiak-Baldys, F. Simbari, P. Roddy, D. M. Perry, K. Kitatani, C. Luberto, and Y. A. Hannun. 2010. Regulated secretion of acid sphingomyelinase. *J. Biol. Chem.* **285**: 35706–35718.
- Schmitz, G., and M. Grandl. 2007. Role of redox regulation and lipid rafts in macrophages during ox-LDL-mediated foam cell formation. *Antioxid. Redox Signal.* **9**: 1499–1518.



31. Gaus, K., M. Rodriguez, K. R. Ruberu, I. Gelissen, T. M. Sloane, L. Kritharides, and W. Jessup. 2005. Domain-specific lipid distribution in macrophage plasma membranes. *J. Lipid Res.* **46**: 1526–1538.
32. Garin, J., R. Diez, S. Kieffer, J-F. Dermine, S. Duclos, E. Gagnon, R. Sadoul, C. Rondeau, and M. Desjardins. 2001. The phagosome proteome. *J. Cell Biol.* **152**: 165–180.
33. Silva, L. C., A. H. Futerman, and M. Prieto. 2009. Lipid raft composition modulates sphingomyelinase activity and ceramide-induced membrane physical alterations. *Biophys. J.* **96**: 3210–3222.
34. Walton, K. A., B. G. Gugi, M. Thomas, R. J. Basseri, D. R. Eliav, R. G. Salomon, and J. A. Berliner. 2006. A role for neutral sphingomyelinase activation in the inhibition of LPS action by phospholipid oxidation products. *J. Lipid Res.* **47**: 1967–1974.
35. Andreyev, A. Y., E. Fahy, Z. Guan, S. Kelly, X. Li, J. G. McDonald, S. Milne, D. Myers, H. Park, A. Ryan, et al. 2010. Subcellular organelle lipidomics in TLR-4-activated macrophages. *J. Lipid Res.* **51**: 2785–2797.
36. Li, X., K. A. Becker, and Y. Zhang. 2010. Ceramide in redox signaling and cardiovascular diseases. *Cell. Physiol. Biochem.* **26**: 41–48.
37. Mansat-de Mas, V., C. Bezombes, A. Quillet-Mary, A. Bettaieb, A. D. T. D'orgeix, G. Laurent, and J-P. Jaffr zou. 1999. Implication of radical oxygen species in ceramide generation, c-Jun N-terminal kinase activation and apoptosis induced by daunorubicin. *Mol. Pharmacol.* **56**: 867–874.
38. Bezombes, C., A. D. Thonel, A. Apostolou, T. Louat, J-P. Jaffr zou, G. Laurent, and A. Quillet-Mary. 2002. Overexpression of protein kinase Cz confers protection against antileukemic drugs by inhibiting the redox-dependent sphingomyelinase activation. *Mol. Pharmacol.* **62**: 1446–1455.